State and Parameter Estimation in Dynamic Real-Time Optimization with Embedded MPC

José Matias, Anthony W. K. Quarshie, Andrew Solano, Christopher L. E. Swartz [1]

* *Department of Chemical Engineering, McMaster University, 1280 Main Street West, Hamilton, Ontario, Canada, L8S 4L7*

Abstract: The goal of dynamic real-time optimization (DRTO) applications is to compute an optimal operational trajectory for a plant by generating set-points for the lower-level control algorithm to track. This approach can be further improved by directly incorporating the control algorithm (such as Model Predictive Control, MPC) into a closed-loop DRTO (CL-DRTO). By doing so, CL-DRTO can predict both the plant and controller responses to set-point adjustments, enhancing the performance of the entire system. However, CL-DRTO schemes require a mechanism to utilize plant measurements to adapt the model to the current plant conditions. Otherwise, the decisions will be based on a nominal model and are likely to be suboptimal. This study proposes a plant feedback scheme using an extended Kalman filter within a CL-DRTO framework that embeds an MPC model. In this novel model adaptation approach in the context of CL-DRTO, not only the states and parameters of the plant model are updated but also the embedded linear MPC model, which is adapted via an output disturbance scheme. Moreover, by adding input constraints to the CL-DRTO problem, this formulation allows a simplified representation of the MPC solution at the CL-DRTO level without directly accounting for input constraints at the MPC level, which reduces computation time. The efficacy of the proposed CL-DRTO approach is demonstrated through application to a multi-input multi-output CSTR where a critical parameter is not measurable.

Keywords: Dynamic Optimization; Model Predictive Control; Nonlinear Systems; Kalman Filtering; Real-time Control

1. INTRODUCTION

Chemical processes are required to respond to frequent changes in external conditions, including product demand, utility costs, and raw material cost and availability. Optimizing such facilities is critical, but often complex since they have design limitations, operational goals, and local control objectives to account for.

Dynamic real-time optimization (DRTO) algorithms can be used for this task. Traditional RTO schemes based on steady-state models yield suboptimal operation in the face of rapidly changing conditions, leading to the development of DRTO schemes that incorporate a dynamic plant model (Tosukhowong et al., 2004). DRTO computes economically optimal trajectories over a prediction horizon, which are then sent to a model predictive control (MPC) layer as set-point trajectories. Then, MPC independently determines the input moves to track these trajectories by solving its own optimization problem. The MPC layer affects the plant dynamic conditions of the plant during transition; thus, taking MPC into account at the DRTO level can improve the overall economics of the plant. Jamaludin and Swartz (2017) included the MPC optimization sub-problems within the DRTO problem formulation, and showed that taking the closed-loop (CL) prediction of MPC behavior into account can significantly improve the economic performance over a similar DRTO that does not take into accopunt the impact of the control system on the plant's dynamic response.

However, in any real applications, the MPC and CL-DRTO layers are affected by disturbances causing plant-model mismatch. There are various approaches to dealing with these issues. While bias updating would be considered standard practice in CL-DRTO literature, its method simply applies a correcting 'bias" term to compensate for a poor model or noisy measurements. Even when working successfully, bias updating cannot predict the true value of the states, and parameters that are not known to the control architecture. The extended Kalman filter can estimate these states as well as unknown parameters, and offers a promising alternative to bias updating in closed-loop DRTO.

This work explores the extended Kalman filter estimation as a method of dealing with disturbances, noise, and the plant-model mismatch in the context of CL-DRTO. In the proposed case-study, we assume that a critical parameter of the system is unknown and not measurable. Our results indicate that continuously estimating model parameters

[1] Corresponding author (e-mail: swartzc@mcmaster.ca)

and states via an EKF enables the CL-DRTO to effectively optimize the nonlinear plant.

Within the CL-DRTO framework, the MPC solution is applied to the nonlinear plant model to predict its response to control actions, allowing the plant model outputs at the DRTO level to serve as surrogate measurements for the embedded MPC in calculating the next manipulated variable value.

2. RELATION TO PREVIOUS WORK

The hierarchical decision-making structure in industrial plants, Fig. 1, separates decisions by time scale to manage complexity effectively. Scheduling focuses on production decisions over a medium-term time frame. By contrast, DRTO integrates scheduling goals into actionable decisions in real-time. Further down, MPC adjusts operations dynamically (Darby et al., 2011).

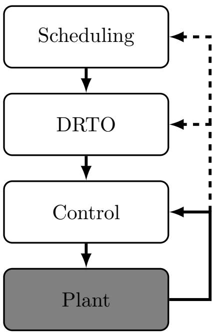

Fig. 1. Plant decision hierarchy. Dotted lines indicate that the plant-feedback is not done as frequently, or not done at all. If no feedback system is in place, decisions are made based on a nominal model.

If the time scale between layers is not clearly separable, there are incentives for considering the behavior of multiple layers simultaneously. For example, if the control system is detuned to achieve a slow and smooth response in systems with significant time delay, the time separation scale between the control response and the DRTO layer response may be significantly reduced. Here, methods like closed-loop DRTO (Jamaludin and Swartz, 2017) become interesting and improve the performance of the hierarchy above.

In the same spirit, different works have considered the behavior of multiple layers at the DRTO/Scheduling level. For example: Jamaludin and Swartz (2017) combined DRTO and constrained MPC; Li and Swartz (2018) and Li and Swartz (2019) studied the integration of DRTO with distributed MPC systems; and Dering and Swartz (2024), Kelley et al. (2022), and Remigio and Swartz (2020) have integrated scheduling and control. However, none of these studies employed any form of estimator, and used bias updating to provide feedback to the DRTO or assumed full-state feedback.

To help models improve their accuracy, dynamic state and parameter estimation can be used in CL-DRTO, such as in Matias and Swartz (2023); however Matias and Swartz (2023) only demonstrated this setup for PI-controlled plants. This type of plant feedback has not yet been tested on CL-DRTO combined with MPC setups. This is particularly interesting for MPC controllers with a disturbance model, as the disturbance term must converge while the estimated parameters converge to their true value, and the interaction may impact control.

3. PRELIMINARIES

3.1 Background

Consider a plant represented by a nonlinear model:

$$\begin{aligned} \dot{\boldsymbol{x}}(t) &= \boldsymbol{f}(\boldsymbol{x}(t), \boldsymbol{u}(t); \boldsymbol{\theta}(t)) \\ \boldsymbol{y}(t) &= \boldsymbol{g}(\boldsymbol{x}(t)) \end{aligned} \tag{1}$$

where $\boldsymbol{x}$, $\boldsymbol{u}$, $\boldsymbol{y}$, and $\boldsymbol{\theta}$ represent the model states, inputs, outputs, and parameters, respectively, with dimensions n_x, n_u, n_y, and n_θ. $\boldsymbol{f}$ and $\boldsymbol{g}$ are functions that represent the state dynamic evolution, and the mapping of the states to the model outputs.

In practice, this nonlinear model can be computationally expensive to evaluate, and it is desirable to approximate its behavior using a linearized state space model. Furthermore, it is convenient to convert the continuous model into a discretized version. The equations describing the discrete linearized model are given below:

$$\begin{aligned} \bar{\boldsymbol{x}}_{k+1} &= A^h_{\boldsymbol{x},\boldsymbol{\theta}}, \bar{\boldsymbol{x}}_k + B^h_{\boldsymbol{x},\boldsymbol{\theta}} \bar{\boldsymbol{u}}_k \\ \bar{\boldsymbol{y}}_k &= C^h_{\boldsymbol{x},\boldsymbol{\theta}} \bar{\boldsymbol{x}}_k \end{aligned} \tag{2}$$

in which the matrices A, B, and C represent the linearized version of the nonlinear model in Eq. (1). The functions $\boldsymbol{f}$ and $\boldsymbol{g}$ are linearized around a specified steady state value. The bar above the variables indicates that the variables are expressed in deviation form from this steady-state. The superscript h indicates the discretization step, and subscripts $\boldsymbol{x}$ and $\boldsymbol{\theta}$ represent the state and parameters around which the linearization is performed.

3.2 MPC

Model predictive controllers predict future dynamics over a set horizon length N_p^{MPC}, using predictions to calculate optimal control actions that best track a set-point trajectory. For obtaining an offset-free performance, the MPC controller implemented here uses a disturbance term as in Maciejowski (2001):

$$\begin{aligned} \begin{bmatrix} \bar{\boldsymbol{x}}^{\mathrm{MPC}}_{k+1} \\ \boldsymbol{d}_{k+1} \end{bmatrix} &= \begin{bmatrix} A^{\mathrm{MPC}}_{\boldsymbol{x}_i,\boldsymbol{u}_i,\boldsymbol{\theta}_n} & 0 \\ 0 & I \end{bmatrix} \begin{bmatrix} \bar{\boldsymbol{x}}^{\mathrm{MPC}}_{k} \\ \boldsymbol{d}_{k} \end{bmatrix} + \begin{bmatrix} B^{\mathrm{MPC}}_{\boldsymbol{x}_i,\boldsymbol{u}_i\boldsymbol{\theta}_n} \\ 0 \end{bmatrix} \bar{\boldsymbol{u}}_k \\ \bar{\boldsymbol{y}}_k &= \begin{bmatrix} C^{\mathrm{MPC}}_{\boldsymbol{x}_i,\boldsymbol{u}_i\boldsymbol{\theta}_n} & I \end{bmatrix} \begin{bmatrix} \bar{\boldsymbol{x}}^{\mathrm{MPC}}_{k} \\ \boldsymbol{d}_{k} \end{bmatrix} \end{aligned} \tag{3}$$

Here the superscript *MPC* indicates that matrices were discretized at the MPC execution rate. The states also receive the superscript to differentiate them from the DRTO plant model states, which will be explained later. The linearization is done at an initial steady state ($\boldsymbol{x}_i$,$\boldsymbol{u}_i$) and the nominal parameters, $\boldsymbol{\theta}_n$; hence, the MPC matrices do not change with time. Given a set-point tractory at k_0

$$\tilde{\boldsymbol{y}}^{SP}_{k_0} = [\bar{\boldsymbol{y}}^{SP,T}_{k_0}, \bar{\boldsymbol{y}}^{SP,T}_{k_0+1}, \ldots, \bar{\boldsymbol{y}}^{SP,T}_{k_0+N_p^{\mathrm{MPC}}-1}]^T,$$

the unconstrained MPC problem can be analytically solved for control actions over the entire prediction horizon as in, for example, Li and Swartz (2018). The analytical solution takes form of:

$$\Delta\tilde{\boldsymbol{u}}_{k_0} = K_{\mathrm{MPC}}\left(\tilde{\boldsymbol{y}}^{SP}_{k_0} - \left(B_1\bar{\boldsymbol{x}}^{\mathrm{MPC}}_{k_0} + B_2\bar{\boldsymbol{u}}_{k_0-1} + \hat{\boldsymbol{d}}_{k_0}\right)\right) \quad (4)$$

where,

$$\Delta\tilde{\boldsymbol{u}}_{k_0} = [\Delta\bar{\boldsymbol{u}}^T_{k_0}, \Delta\bar{\boldsymbol{u}}^T_{k_0+1}\cdots, \Delta\bar{\boldsymbol{u}}^T_{k_0+N_p^{\mathrm{MPC}}-1}]^T,$$
$$\Delta\bar{\boldsymbol{u}}_k = \bar{\boldsymbol{u}}_k - \bar{\boldsymbol{u}}_{k-1},$$

Note that the vector of inputs

$$\tilde{\boldsymbol{u}}_{k_0} = [\bar{\boldsymbol{u}}^T_{k_0}, \bar{\boldsymbol{u}}^T_{k_0+1}\cdots, \bar{\boldsymbol{u}}^T_{k_0+N_p^{\mathrm{MPC}}-1}]^T$$

can be related to the vector of inputs moves as

$$\tilde{\boldsymbol{u}}_{k_0} = \tilde{M}\Delta\tilde{\boldsymbol{u}}_{k_0} + \tilde{I}\bar{\boldsymbol{u}}_{k_0-1} \quad (5)$$

where

$$\tilde{M} = \begin{bmatrix} I_{n_u} & 0_{n_u} & \cdots & 0_{n_u} \\ I_{n_u} & I_{n_u} & \cdots & 0_{n_u} \\ \vdots & \vdots & \ddots & \vdots \\ I_{n_u} & I_{n_u} & \cdots & I_{n_u} \end{bmatrix}, \quad \tilde{I} = \begin{bmatrix} I_{n_u} \\ I_{n_u} \\ \vdots \\ I_{n_u} \end{bmatrix}$$

with I_{n_u} representing the $n_u \times n_u$ identity matrix, and 0_{n_u} a $n_u \times n_u$ matrix with zeros in all entries. The states $\bar{\boldsymbol{x}}_{\mathrm{MPC},k_0}$ are computed from the nominal MPC model and the disturbance estimate is computed as the difference between the plant measurement $\boldsymbol{y}_p$ and the model output prediction at the same time instant k_0 as in Eq. (6).

$$\hat{\boldsymbol{d}}_{k_0} = [\boldsymbol{d}^T_{k_0}, \boldsymbol{d}^T_{k_0+1}, \ldots, \boldsymbol{d}^T_{k_0+N_p^{\mathrm{MPC}}-1}]^T,$$
$$\boldsymbol{d}_{k_0} = \bar{\boldsymbol{y}}_{p,k_0} - C^{\mathrm{MPC}}_{\boldsymbol{x}_i,\boldsymbol{u}_i\boldsymbol{\theta}_n}\bar{\boldsymbol{x}}^{\mathrm{MPC}}_{k_0} \quad (6)$$

For a detailed description of the matrices K_{MPC}, B_1 and B_2, the reader is referred to Li and Swartz (2018).

3.3 CL-DRTO

A critical component of the solution of CL-DRTO is the incorporation of the MPC algorithm to simulate the expected response of the controller to its chosen set-points. In Jamaludin and Swartz (2017), the input-constrained MPC problem is represented at the DRTO level by its KKT conditions. Here, we use the analytical solution of the unconstrained problem presented in Eq. (4) combined with an input clipping strategy.

Instead of rigorously representing the input clipping as in Baker and Swartz (2004), we take advantage of the fact that the DRTO optimization problem has access to the unconstrained MPC predicted response; thus, the DRTO can constrain its set-points such that the inputs remain in the feasible region, avoiding the need of input clipping.

The resulting CL-DRTO problem can be seen in Eq. (7).

$$\begin{aligned}
&\max_{\tilde{\boldsymbol{y}}^{SP}_j} \quad \sum_{j_0}^{j_0+N_p^{\mathrm{DRTO}}} \Phi(\bar{\boldsymbol{u}}^{\mathrm{DRTO}}_j, \bar{\boldsymbol{x}}^{\mathrm{DRTO}}_j, \bar{\boldsymbol{y}}^{\mathrm{DRTO}}_j)\\
&\text{s.t.}\\
&\bar{\boldsymbol{x}}^{\mathrm{DRTO}}_{j+1} = \boldsymbol{f}(\bar{\boldsymbol{x}}^{\mathrm{DRTO}}_j, \bar{\boldsymbol{u}}^{\mathrm{DRTO}}_j, \hat{\bar{\boldsymbol{\theta}}}_{j_0}) && j \in \mathcal{J}_{j_0}^{j_0+N_p^{\mathrm{DRTO}}-1}\\
&\bar{\boldsymbol{y}}^{\mathrm{DRTO}}_j = \boldsymbol{g}(\bar{\boldsymbol{x}}^{\mathrm{DRTO}}_j) && j \in \mathcal{J}_{j_0}^{j_0+N_p^{\mathrm{DRTO}}}\\
&\bar{\boldsymbol{x}}^{\mathrm{DRTO}}_{j_0} = \hat{\bar{\boldsymbol{x}}}_{j_0}\\
&\bar{\boldsymbol{u}}^{\mathrm{DRTO}}_j = \bar{\boldsymbol{u}}^{\mathrm{MPC}}_{j,0} && j \in \mathcal{J}_{j_0}^{j_0+N_p^{\mathrm{DRTO}}-1}\\
&\Delta\tilde{\boldsymbol{u}}_j = K_{\mathrm{mpc}}\left(\tilde{\boldsymbol{y}}^{SP}_j - \left(B_1\bar{\boldsymbol{x}}^{\mathrm{MPC}}_{j,0} + B_2\bar{\boldsymbol{u}}_{j-1,0} + \boldsymbol{d}^{\mathrm{MPC}}_{j,0}\right)\right) && j \in \mathcal{J}_{j_0}^{j_0+N_p^{\mathrm{DRTO}}-1}\\
&\bar{\boldsymbol{u}}^{\mathrm{MPC}}_{j,l} = \tilde{M}_{(l,:)}\Delta\tilde{\boldsymbol{u}}_j + \tilde{I}_{(l,:)}\bar{\boldsymbol{u}}_{j-1} && l \in \mathcal{L}_0^{N_p^{\mathrm{MPC}}-1} \quad j \in \mathcal{J}_{j_0}^{j_0+N_p^{\mathrm{DRTO}}-1}\\
&\bar{\boldsymbol{x}}^{\mathrm{MPC}}_{j,l+1} = A^{\mathrm{MPC}}_{\boldsymbol{x}_i,\boldsymbol{u}_i,\boldsymbol{\theta}_n}\bar{\boldsymbol{x}}^{\mathrm{MPC}}_{j,l} + B^{\mathrm{MPC}}_{\boldsymbol{x}_i,\boldsymbol{u}_i,\boldsymbol{\theta}_n}\bar{\boldsymbol{u}}^{\mathrm{MPC}}_{j,l} && l \in \mathcal{L}_0^{N_p^{\mathrm{MPC}}-1} \quad j \in \mathcal{J}_{j_0}^{j_0+N_p^{\mathrm{DRTO}}-1}\\
&\bar{\boldsymbol{y}}^{\mathrm{MPC}}_{j,l} = C^{\mathrm{MPC}}_{\boldsymbol{x}_i,\boldsymbol{u}_i,\boldsymbol{\theta}_n}\bar{\boldsymbol{x}}^{\mathrm{MPC}}_{j,l} && l \in \mathcal{L}_0^{N_p^{\mathrm{MPC}}} \quad j \in \mathcal{J}_{j_0}^{j_0+N_p^{\mathrm{DRTO}}}\\
&\bar{\boldsymbol{x}}^{\mathrm{MPC}}_{j,0} = \bar{\boldsymbol{x}}^{\mathrm{MPC}}_{j-1,N_p^{\mathrm{MPC}}} && j \in \mathcal{J}_{j_0+1}^{j_0+N_p^{\mathrm{DRTO}}-1}\\
&\boldsymbol{d}^{\mathrm{MPC}}_{j,0} = \bar{\boldsymbol{y}}^{DRTO}_j - \bar{\boldsymbol{y}}^{\mathrm{MPC}}_{j,0} && j \in \mathcal{J}_{j_0+1}^{j_0+N_p^{\mathrm{DRTO}}-1}\\
&\bar{\boldsymbol{u}}_{\min} \leq \bar{\boldsymbol{u}}_{j,l} \leq \bar{\boldsymbol{u}}_{\max} && l \in \mathcal{L}_0^{N_p^{\mathrm{MPC}}-1} \quad j \in \mathcal{J}_{j_0}^{j_0+N_p^{\mathrm{DRTO}}-1}\\
&\Delta\tilde{\boldsymbol{u}}_{\min} \leq \Delta\tilde{\boldsymbol{u}}_j \leq \Delta\tilde{\boldsymbol{u}}_{\max} && j \in \mathcal{J}_{j_0}^{j_0+N_p^{\mathrm{DRTO}}-1}\\
&\tilde{\boldsymbol{y}}_{\mathrm{sp},\min} \leq \tilde{\boldsymbol{y}}^{SP}_j \leq \tilde{\boldsymbol{y}}_{\mathrm{sp},\max} && j \in \mathcal{J}_{j_0}^{j_0+N_p^{\mathrm{DRTO}}-1}\\
&\Delta\tilde{\boldsymbol{y}}_{\mathrm{sp},\min} \leq \Delta\tilde{\boldsymbol{y}}^{SP}_j \leq \Delta\tilde{\boldsymbol{y}}_{\mathrm{sp},\max} && j \in \mathcal{J}_{j_0}^{j_0+N_p^{\mathrm{DRTO}}-1}
\end{aligned} \quad (7)$$

In Eq. (7), Φ is an economic objective function. To represent the intermediary time steps, we use the notation $\mathcal{J}_a^b := \{j \mid a \le j \le b, j \in \mathbb{Z}_0^+\}$. The subscript $(l, :)$ indicates that the l^{th} row of the matrix is used in the operation. Note that we start counting from index 0. Finally, the superscripts *DRTO* and *MPC* indicate that the linearized model was discretized using the DRTO sampling time and MPC sampling time, respectively.

3.4 Plant Feedback Mechanism: Extended Kalman Filter

Typically, the states and parameters of the plant model are unknown (in Eq. (7), $\hat{\tilde{\boldsymbol{\theta}}}_{j_0}$ and $\hat{\tilde{\boldsymbol{x}}}_{j_0}$) and an estimator needs to be used to obtain their true values. Kalman filter estimation can be used to calculate the estimated states and unknown parameters of a model, a helpful tool in systems where not all desired states are measurable or where measurements may be inaccurate due to noise or other disturbances.

The Extended Kalman Filter (EKF) is preferred over the standard Kalman Filter when dealing with nonlinear systems. While the Kalman Filter assumes linear dynamics and Gaussian noise, the EKF linearizes the nonlinear model (shown in Eq. (1)) around the current state and parameter estimates by using a first-order Taylor expansion. This allows it to handle the nonlinearity in the process or measurement models, making it suitable for our applications. A detailed description of an EKF can be found in Walter et al. (1997).

3.5 Proposed Architecture

While the individual control elements used here (DRTO, MPC, Kalman filter Estimation, etc.) are not novel on their own, using them together is indeed novel for CL-DRTO. Adding state and parameter estimation to the CL-DRTO can improve its robustness in practical use where not all variables are measurable. The value of the MPC disturbance vector is also updated within the DRTO to improve the accuracy of the DRTO optimization. Figure 2 shows the information flow in the proposed architecture.

4. CASE STUDY

The case study used here is a multi-input multi-output CSTR. The parameters governing the system dynamics were obtained from Li et al. (2016). The inlet flowrate (F) and heat to the reactor (Q) are the manipulated variables and the reactant concentration in the CSTR (C_A) and reactor temperature (T) are the controlled variables. To test the estimator, a heater efficiency term (η) has been added to the original model. The nonlinear equations governing the CSTR are:

$$\frac{dC_A}{dt} = \frac{F}{V_R}(C_{A,in} - C_A) - k_0 e^{-\frac{E}{RT}} C_A^2 \tag{8}$$

$$\frac{dT}{dt} = \frac{F}{V_R}(T_{in} - T) - \frac{\Delta H k_0}{\rho_R C_p} e^{-\frac{E}{RT}} C_A^2 + \frac{\eta Q}{\rho_R C_p V_R} \tag{9}$$

where we assume that both the inlet flow rate F and the heater power Q can be manipulated ($n_u = 2$), and both states C_A and T can be measured ($n_x = n_y = 2$) without noise. We assume that true efficiency value ($\theta := \eta_{true} = 0.9$) is unknown and needs to be estimated. The initial condition for the simulation is provided in Table 1.

Table 1. Parameters used to simulate a CSTR for the case study based on Li et al. (2016)

Symbol	Description	(Initial) Value	Units
$C_{A,i}$	Conc. of A in CSTR	0.339	kmol/m^3
T_i	Temperature of CSTR	545	K
F_i	Inlet Flowrate	5	m^3/h
Q_i	Heater Power	99,840	kJ/h
$C_{A,in}$	Inlet Conc. of A	3.5	kmol/m^3
T_{in}	Inlet Temperature	300	K
k_0	Pre-exponential rate factor	8.46×10^6	m^3/kmol-h
E	Activation Energy	5×10^4	kJ/kmol
R	Ideal Gas Constant	8.314	kJ/kmol-K
ρ_R	Density of fluid in CSTR	1000	kg/m^3
C_p	Heat capacity of fluid in CSTR	0.231	kJ/kg-K
V_R	Reactor fluid volume	1.0	m^3
ΔH	Heat of reaction	-1.16×10^4	kJ/kmol
η_{true}	Heater true efficiency	0.9	——
η_n	Heater nominal efficiency	0.95	——

The MPC and DRTO are discretized based on their respective sampling times $h_{\text{MPC}} = 2$ minutes and $h_{\text{DRTO}} = 10$ minutes. The prediction horizons are represented as multiples of the sampling times, $N_P^{\text{MPC}} = 3$ and $N_P^{\text{DRTO}} = 10$.

The function Φ in Eq. (7) represents economic performance by using the profitability approximation proposed by Li et al. (2016):

$$\varphi = \alpha F(C_{A0} - C_A) - \gamma Q^2, \tag{10}$$

where $\alpha = 10^5$ \$/kmol and $\gamma = 10^{-7}$ \$ $\cdot$ h/ kJ^2. The units of α and γ are such that φ units are in 10^6 \$/h. The bounds used in the DRTO problem, Eq. (7), are shown in Table 2.

Table 2. Constraints applied to the DRTO

State	Lower Bound	Upper Bound	Units
C_A	0.1	3.5	kmol/m^3
T	400	700	K
F	0	7	m^3/h
Q	0	220000	kJ/h
ΔF	-0.8	-0.8	m^3/h
ΔQ	-80000	80000	kJ/h
$C_{A,sp}$	0	3.5	kmol/m^3
T_{sp}	400	700	K
$\Delta C_{A,sp}$	- 0.2	0.2	kmol/m^3
ΔT_{sp}	-30	30	K

5. RESULTS AND DISCUSSION

Improving economic performance is a the main operational goal, so the CL-DRTO architecture was evaluated for its ability to meet an economic objective.

Figure 3 shows the parameter (η) and states (C_A, T). In the plots, the plant values (black) are compared to the estimated values (green). Figure 4 shows the manipulated variables (F, Q) used in the objective function from Equation 10 and the economic performance. The economic performance is evaluated as the difference between the computed instantaneous φ value and the value obtained at the initial steady state.

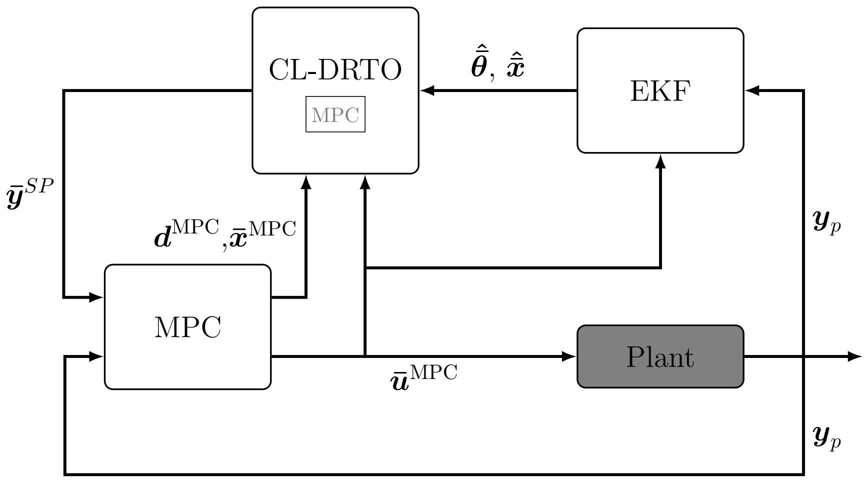

Fig. 2. Information flow diagram of proposed control architecture using DRTO, MPC, and EKF Estimation

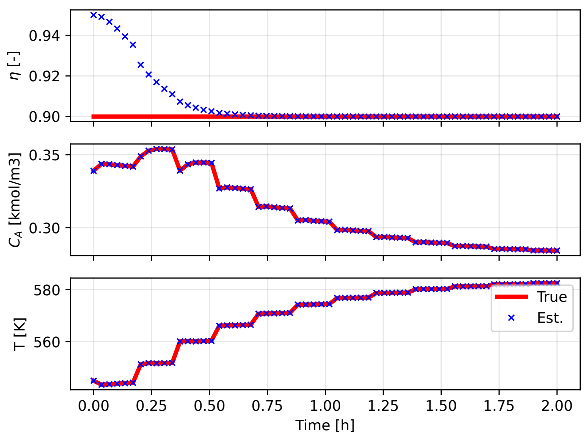

Fig. 3. Estimated states and parameters.

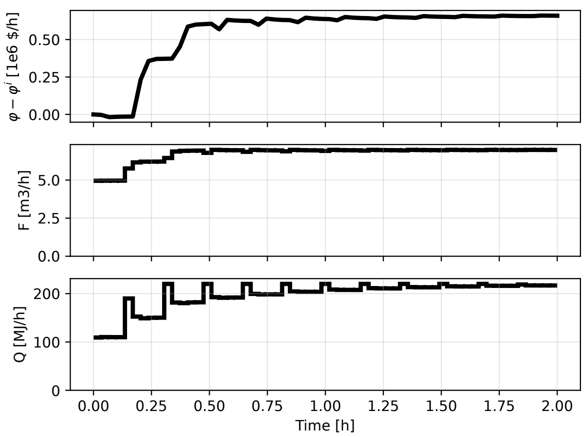

Fig. 4. Manipulated variables and economic criterion.

The performance shown in Figures 3 and 4 indicates several interesting findings. First, the Extended Kalman Filter (EKF) is able to effectively track the true parameter values. The state estimation itself is not critical here as both states are assumed to be measured. The estimation step converges relatively quickly for this case study, and the system converges to a new steady state, as illustrated in the top plot of Figure 4. While the heat input trajectory shows some sharp variation, this reflects only marginally in the objective function trajectory.The plant response is monotonic, with the temperature increasing and the concentration decreasing. The upward trend of the objective function is explained by the CL-DRTO finding an optimal steady state, given the initial suboptimal steady-state point. As such, the framework not only handles varying parameter values due to the estimation, but it also drives the plant to an optimal steady state.

The set-point determination by the CL-DRTO layer, as shown in Eq. 7, also constrains input and setpoint movement in addition to the constraints on inputs. This is made possible by the closed-loop response set-up in the CL-DRTO, which uses a nonlinear plant model. These structures are important given that an unconstrained linear MPC is used to control the nonlinear plant. The effectiveness of these structures is inferred from the absence of constraint violations in the implementation of set-points at the plant level. Note, however, that these results are achieved through appropriate application of constraint bounds on inputs, and on set-point and input changes at the CL-DRTO layer. Without these constraints, larger oscillations could be introduced into the inputs, and in turn possibly affecting the states and outputs. In demonstrating the effectiveness of framework, the unconstrained MPC does not eliminate the oscillations observed for the heat input despite a nonzero move suppression penalty. The controller moves to promptly attain the newly computed set-points from the CL-DRTO, thus observed spikes. More gradual changes could potentially be implemented by a constrained MPC which directly implements hard constraints on input moves.

Embedding unconstrained MPC to predict closed-loop the response of the nonlinear plant at the CL-DRTO layer in conjunction with constraints on inputs, set-points moves and input moves is shown to be an effective strategy. In this study, it is observed that the framework offers a good compromise between computational performance improvement and available handles for effective control.

6. CONCLUSION

This study proposes integrating an Extended Kalman Filter (EKF) with Closed-Loop Dynamic Real-Time Optimization (CL-DRTO) for operation of a plant under the control of a Model Predictive Control (MPC) system. The EKF successfully estimates states and parameters, enabling the CL-DRTO to make accurate predictions and send optimal set-points to the MPC.

This study demonstrates the effectiveness of combining DRTO, MPC, and Kalman filter layers. This approach can handle nonlinear behavior through incorporation of a nonlinear plant model at the DRTO level. Future research should explore the full potential of this approach, especially for large-scale systems of industrial complexity. Problems of such scale would require exploration of dynamic surrogate models for tractable formulations. Other avenues for exploration include consideration of computationally efficient implementation of constrained MPC and estimating multiple unknown parameters.

ACKNOWLEDGEMENTS

The authors gratefully acknowledge support from the Ontario Research Fund - Research Excellence (ORF-RE) Award RE09-058, and the McMaster Advanced Control Consortium (MACC).

REFERENCES

Baker, R. and Swartz, C.L.E. (2004). Rigorous handling of input saturation in the design of dynamically operable plants. *Industrial & engineering chemistry research*, 43(18), 5880–5887.

Darby, M.L., Nikolaou, M., Jones, J., and Nicholson, D. (2011). Rto: An overview and assessment of current practice. *Journal of Process control*, 21(6), 874–884.

Dering, D. and Swartz, C.L.E. (2024). Integration of scheduling and control for plants controlled by distributed mpc systems. *Industrial & Engineering Chemistry Research*, 63(27), 12016–12034.

Jamaludin, M.Z. and Swartz, C.L.E. (2017). Approximation of closed-loop prediction for dynamic real-time optimization calculations. *Computers & Chemical Engineering*, 103, 23–38.

Kelley, M.T., Tsay, C., Cao, Y., Wang, Y., Flores-Cerrillo, J., and Baldea, M. (2022). A data-driven linear formulation of the optimal demand response scheduling problem for an industrial air separation unit. *Chemical Engineering Science*, 252, 117468.

Li, H. and Swartz, C.L.E. (2018). Approximation techniques for dynamic real-time optimization (DRTO) of distributed mpc systems. *Computers & Chemical Engineering*, 118, 195–209.

Li, H. and Swartz, C.L.E. (2019). Dynamic real-time optimization of distributed mpc systems using rigorous closed-loop prediction. *Computers & Chemical Engineering*, 122, 356–371.

Li, X., Zhang, L., Nakaya, M., and Takenaka, A. (2016). Application of economic MPC to a CSTR process. In *2016 IEEE Advanced Information Management, Communicates, Electronic and Automation Control Conference (IMCEC)*, 685–690. IEEE.

Maciejowski, J.M. (2001). *Predictive Control with Constraints*. Prentice Hall.

Matias, J. and Swartz, C.L.E. (2023). State and parameter estimation in dynamic real-time optimization with closed-loop prediction. In *Computer Aided Chemical Engineering*, volume 52, 1867–1872. Elsevier.

Remigio, J.E. and Swartz, C.L.E. (2020). Production scheduling in dynamic real-time optimization with closed-loop prediction. *Journal of Process Control*, 89, 95–107.

Tosukhowong, T., Lee, J.M., Lee, J.H., and Lu, J. (2004). An introduction to a dynamic plant-wide optimization strategy for an integrated plant. *Comput. Chem. Eng.*, 29(1), 199–208.

Walter, E., Pronzato, L., and Norton, J. (1997). *Identification of parametric models from experimental data*, volume 1. Springer.